Implication of Secondary Geodynamic Phenomena on Co-seismic Interferometric Coherence

Parcharidis Is. [(1)], Foumelis M. [(2)], Lekkas E. [(3)] & Segou M. [(3)]

[(1)] Harokopio University of Athens, Dept. of Geography, El. Venizelou 70 Kallithea, 17670 Athens, Greece, parchar@hua.gr
[(2)] National and Kapodistrian University of Athens, Faculty of Geology, Dept. of Geophysics – Geothermics, mfoum@geol.uoa.gr
[(3)] National and Kapodistrian University of Athens, Faculty of Geology, Dept. of Dynamic Tectonic & Applied Geology, elekkas@geol.uoa.gr, msegou@geol.uoa.gr

ABSTRACT

On August 14, 2003 a strong earthquake (Mw 6.4) stroke the island of Lefkada. The epicenter was located off shore, about 30 km WNW of the town of Lefkada. A significant number of earthquake-related phenomena such as ground fissures, landslides, rockfalls, soil liquefaction and coastline changes were observed. Moderate damages due to geotechnical events were reported at the western and northern parts of the island. Road network and harbours across the island were heavily affected. Loss of coherence, a major limitation of DInSAR technique, occurs when the physical and/or geometrical nature of the ground changes (vegetation, water, ploughed field etc.), and as a consequence the stability of the phase signal is lost. Thus interferometric coherence is considered to be a measure of the quality of the interferometric analysis. The present paper is focused on the degree of degradation of interferometric coherence caused by earthquake-triggered geodynamic phenomena. The study was based on coherence image produced by applying the two passes interferometric technique using two ENVISAT ASAR scenes forming a co-seismic interferometric pair. Although a fringe pattern was clearly recognized as the majority of the triggered phenomena occurred in that specific area, considerable noise is been inherited in the interferogram due to the lack of coherence. A correlation analysis between coherence values and the location of secondary phenomena recorded through field observation was performed.

1 INTRODUCTION

The SAR interferometry uses the information provided from the phase of two SAR images acquired on two consequences passes to generate interferometric images by differencing the phase values of the images. Eventually range changes along the line of sight (LOS) between the two acquisitions could generate interferometric phase, which could be attributed to various sources the main of which include local topography (φ_{topo}), displacement of surface scatterers (φ_{def}), atmospheric perturbations (φ_{atm}) that causes delays in the signal propagation and noise (φ_{noise}) (Eq. 1).

$$\varphi_{meas} = \varphi_{topo} + \varphi_{def} + \varphi_{flat} + \varphi_{atm} + \varphi_{noise} \quad (1)$$

With differential interferometry the interest is focuses in φ_{deform}. The noise presented in an interferometric image is due to the loss of coherence between the two scenes. The interferometric coherence represents a measurement of the stability of the backscattered SAR signal over an area of interest. It is widely used either as a 'reliability map' of the interferogram (e.g. a pixel-to-pixel measure of SNR), or for changes detection and classification. The loss of coherence can seriously hamper interferometric analysis [1].
There are two main parameters that affect the coherence between the images. The first concerns changes in the properties of ground surface and especially those related to land cover types and are proportional to the time separation (temporal decorrelation). The second parameter concerns the differences in the position of satellite at the moment of acquisition (spatial decorrelation). According to [2], the main design and environmental parameters that influence the potential applications and pose limitations in deformation monitoring are summarized in Table 1.
Other factors that could affect the coherence are related to the data processing like:

i. Uncompensated topography, a differential interferogram is by definition processed in conjunction with a Digital Elevation Model (DEM), such that the effects of topography are removed from the output phase image. The magnitude of topographically related errors is thus a function of the quality of the DEM and the accuracy with which it is co-registered to the data set.
ii. The RMS error of the co-registration between the SAR pair and between the SAR master image and the external DEM (number of tie-points and their spatial distribution, RMS value). Particularly, excellent results have been presented concerning the detection of the co-seismic deformation [3, 4, 5, 6, 7].

Table 1.

Design parameters	Environmental parameters
Wavelength (λ) of the radar signal	Atmosphere (A)
Distance between the satellites (Bperp)	Surface (S)
Temporal baseline (Bt)	Deformation (D)
Number of images (N)	
Incident angle (θ)	

The present study aims to reveal that other extra parameters not necessary related to the parameters mentioned above, but to the seismic event itself, could affect the results of the InSAR co-seismic deformation monitoring. These parameters are related to the nature of the seismic event and the secondary geodynamic phenomena triggered by it. An attempt to investigate the degree of degradation of interferometric coherence caused by earthquake-triggered geodynamic phenomena is the aim of this paper. In this case the interferometric results of Lefkada island (Ionian Sea, Western Greece) earthquake on 14-8-2003 have been taken under investigation.

2 LEFKADA EARTHQUAKE AND RELATED GEODYNAMIC PHENOMENA

The west segment of the Hellenic Arc, including the Ionian Islands, is the more active plate margin of the Mediterranean area, with frequent occurrence of large earthquakes (Fig. 1). The most prominent geotectonic feature is the Hellenic Trench, where the oceanic lithosphere subducts under the Aegean microplate giving large intermediate-depth earthquakes many of them reported since the historic times. However the Ionian Islands, and especially the region of Lefkada and Cephallonia islands, are characterized by shallow seismicity, which is associated for many researchers with the right-lateral strike slip faulting along the forementioned islands. Reference [8] was the first to notice the existence of such transform motions based on focal mechanism data. Last decade the above phenomenon received confirmation with means of GPS data [9, 10]. Many researchers [11, 12, 13, 14, 15] have studied this pronounced feature in geodynamic and tectonic context.

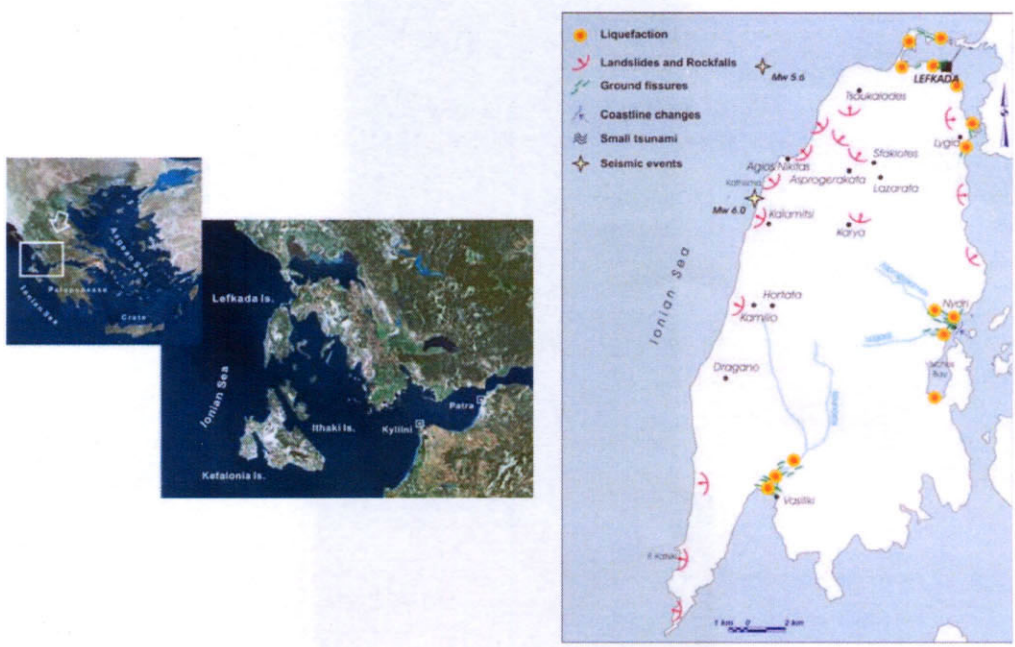

Fig. 1. Location map of the study area (left) and geological and geotechnical effects of the Lefkada earthquake (right).

The Cephallonia Transform Fault Zone (from here after CTFZ) has two main segments, the Lefkada Segment in the north and the Cephallonia segment to the south. Both rupture across the west coast of these islands with a small change in their directions; a more easterly azimouth in the Cephallonia segment. Since 1612 , 16 strong (M≥6) earthquakes have been related to this fault. Prior to Lefkada earthquake the two strongest shocks during the pre-instrumental era were in 1914 (M 6.3) and 1948 (M 6.5) causing broad damages [16]. Reference [12] studied especially the Lefkada

segment described as a zone of ~40km length and a width of ~15km, in N-NE direction, dips to the E-SE characterized by dextral strike slip motion combined with a small thrust component. Reference [12] showed that the typical focal mechanism for the Lefkada segment is strike 14°, dip 65° and rake 167°.
On 14 August 2003 (05:14GMT) a moderate earthquake with magnitude Mw 6.2 occurred on the north part of the Lefkada island with its epicenter lying on the north edge of the Lefkada Segment. According to the interpretation of Benetatos et al. (2005), the main shock was characterized as a multiple-source event. The rupture initiated at the northernmost part of the Lefkada segment as a normal faulting sub-event (Mw 5.6), then in 2.5s propagated ~7km southwards, where the second sub-event (Mw 6.0) occurred. A third event, corresponding to seismic moment Mw 5.8, was located 33km SSW of the second sub-event and close to the southern edge of the Lefkada segment. The two stronger sub-events have focal mechanisms, supporting the reactivation of the Lefkada segment of CTFZ whereas the first event maybe related with normal faulting almost perpendicular to the major CTFZ, confirming the complicated structural pattern of deformation characterizing SW Greece [17] .

Fig. 2. Landslides and rockfalls in the study area triggered by the earthquake.

The maximum intensity has been evaluated as Io=VIII (EMS) near the town of Lefkada, while VI to VII+ intensities have been evaluated at many other villages of the island. The most characteristic earthquake related geodynamic phenomena were extensive ground failures like rock falls, soil liquefactions, subsidense, densification, ground cracks and landslides (Fig. 1). Liquefaction phenomena dominate the broader area of the coastal zone near the town of Leukada. The evaluation of this earthquake effect by reference [18] indicate that a silty sandy layer, which lies beneath the artificial fill in the zone above had liquefied during Lefkada earthquake. Landslides were mainly observed at the central and northern part of the island, as well at the steep western coastal zone near the villages of Tsoukalades, Agios Nikitas. Kathisma, Kalamitsi, Chortata, Dragano, Komilio (Fig. 2). The steep morphology of the west coast, observed at the Ionian Islands, due to the active tectonism of the area, and the highly fractured rock mass played an important role in the appearance of such phenomena. Coastline changes accompanied the event in the northern part of the island. Coastline retreat of about 1m to 20m was a result of densification of Holocene deposits, liquefaction and small submarine landslides [19]. It is noteworthy that the above earthquake related geodynamic phenomena are similar to those reported in historical events of 1704, 1914 (Ms 6.3), and 1948 (Ms 6.5).

3 PROCESSING AND ASSESSMENT OF INTERFEROMETRIC RESULTS

After a quarry in the EOLI ESA's scenes database two ERS-like ENVISAT ASAR, Image Mode (IM) scenes I2 (dated 23/03/03 and 12/09/03), forming a suitable interferometric pair (Bp=53m) and covering the entire area affected by the seismic event have been used. The differential interferometric SAR processing and analyses were based on the Atlantis EarthView v. 3.1 software. The two-pass differential interferometry method (or DEM elimination method) was applied. This method employs two SAR images, producing thus one interferogram. To perform the differential one, another interferogram has to be created or synthesized. The synthesized interferogram is generated from an existing Digital Elevation Model (DEM). The synthesized interferogram is then subtracted from the original interferogram, thereby removing all fringes that relate to ground elevation, leaving only fringes that are assumed to represent surface displacements. The phase differences that remain as fringes in the differential interferogram are a result of range changes of any displaced point on the ground (Fig. 3).
In order to proceed with the main interferometric processing, firstly a DEM was generated with 20 meters of resolution and height accuracy of ±4m approximately. The DEM was already geocoded into the Universal Transverse Mercator

(UTM) projection (similar to the SAR and ASAR scenes). Height information contained in the produced DEM was used to remove the topographic component of the phase in the interferograms.

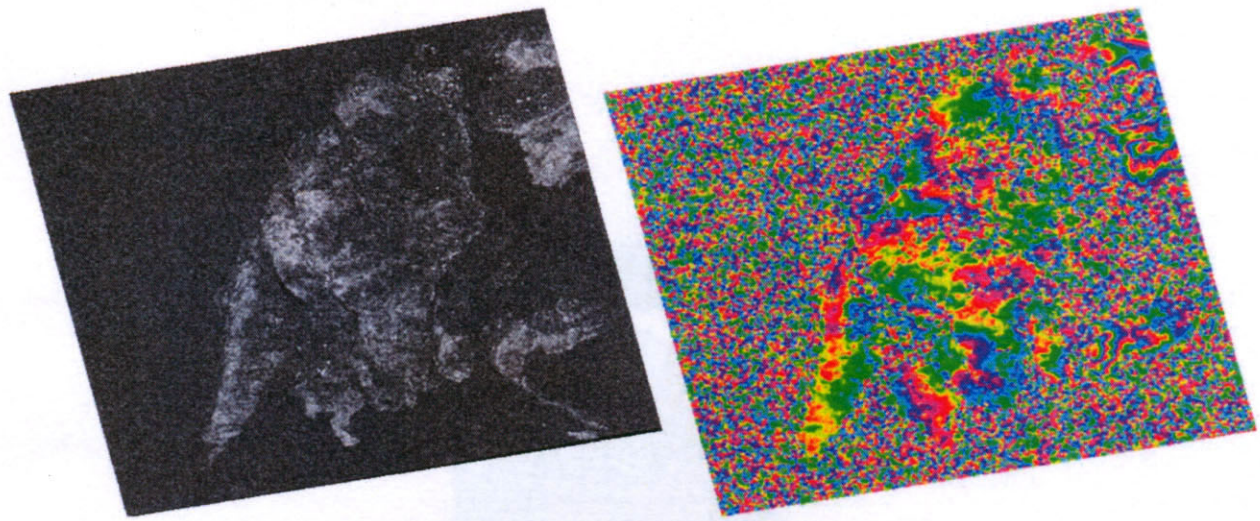

Fig. 3. Interferometric coherence image (left) and corresponding differential interferogram (right) of the 14/08/03 Lefkada earthquake.

The main steps of the processing include co-registration of the master and slave images, validation of the pair for spatial and spectral overlap, co-registration of the external DEM to master at a sub-pixel accuracy, "flat-earth" phase removal, spectral filtering removal of elevation phase contribution using the external DEM, first interferogram production, coherence map generation and estimation, phase unwrapping using the Disk masking Algorithm, slant range change map generation and geocoding into UTM projection. Specifically the phase unwrapping method used in this case was the Iterative Disk Masking (Atlantis patent). This method starts by unwrapping areas of high coherence and then interactively into the low coherence areas. The algorithm begins by masking out both low coherence areas and residues by placing disks of a specific radius over the low coherence and residues. The pixels not masked by the above procedure are unwrapped. In the case of an error all the disks are increased until the remaining unmasked pixels can be unwrapped without an error. The errors are locations where there is a phase discontinuity in the unwrapped image or jump by $>2\pi$ radians.

An accurate investigation of the coherence map, of the interferometric image and the processing characteristics leads to the following remarks. In the coherence image (Fig. 3) dark areas have a low coherence and indicate surface types whose scatter mechanisms or scatter geometry changed during in the time between the two acquisitions. Bright areas have a high coherence and indicate small or no changes in the scatter characteristics. On the island generally the coherence could be classified in two qualitative categories one of low coherence with values between 0.3-0.5 and the other with values between 0.6-0.8. The first is located in the plains where agriculture activities take place and also locally in the slopes of the main relieves. The second is located in the urban center (Lefkada city) as spots for the minor building centers and in the medium and high relieves of the island.

The land displacement patterns due to Lefkada earthquake are possible to extract from the differential interferogram shown in figure 4. However in the plain areas the interferogram is almost noisy due to the low coherence while the phase patterns correspond to mountains areas. One and half fringe is recognized in the northwestern part of the island of semicircular shape, which is extended as linear fringe towards southwest parallel to the western coast. Another less extended fringe is recognized in the northeastern edge of the island close to the Lefkada city. The two fringes are independent to each other, and possibly could be attributed to the two subevents of the main shock. The amount of displacement in a slant range direction is a half of the wavelength for each cycle of phase patterns (28mm).

Taking into consideration the geometric parameters of the interferometric analysis, such as the temporal separation (171 days), decorrelation due to changes of backscatters characteristics was not expected. To support this assumption an NDVI image was calculated using a Landsat 7 ETM+ image acquired at the period cover by the SAR image pair. Low NDVI values at the region of interest indicating the lack of densely vegetated lands indirectly imply the stability of such an area at least at short timescales as the one considered by the used InSAR parirs. In addition topographic phase due to DEM error was to be considered minimal or totally absent as the DEM used is of high resolution and the perpendicular

baseline relatively low (53m). The altitude of ambiguity calculated for the specific interferometric geometry is of 177m, while the difference in elevation in the deformed area covered by the fringe is around 1000m.
Other factors that could introduce such degradation to the InSAR results are the processing parameters. These parameters are mainly related to registration accuracy for master and slave image co-registration as well as to the co-registration of the DEM to the selected master image. In both cases the accuracy achieved as it is described by the RMS error was at a subpixel level. Of great importance is the co-registration error between the DEM and the master which in this case was 0,856 pixels at the X direction (range) and 0,875 at the Y direction (azimuth).

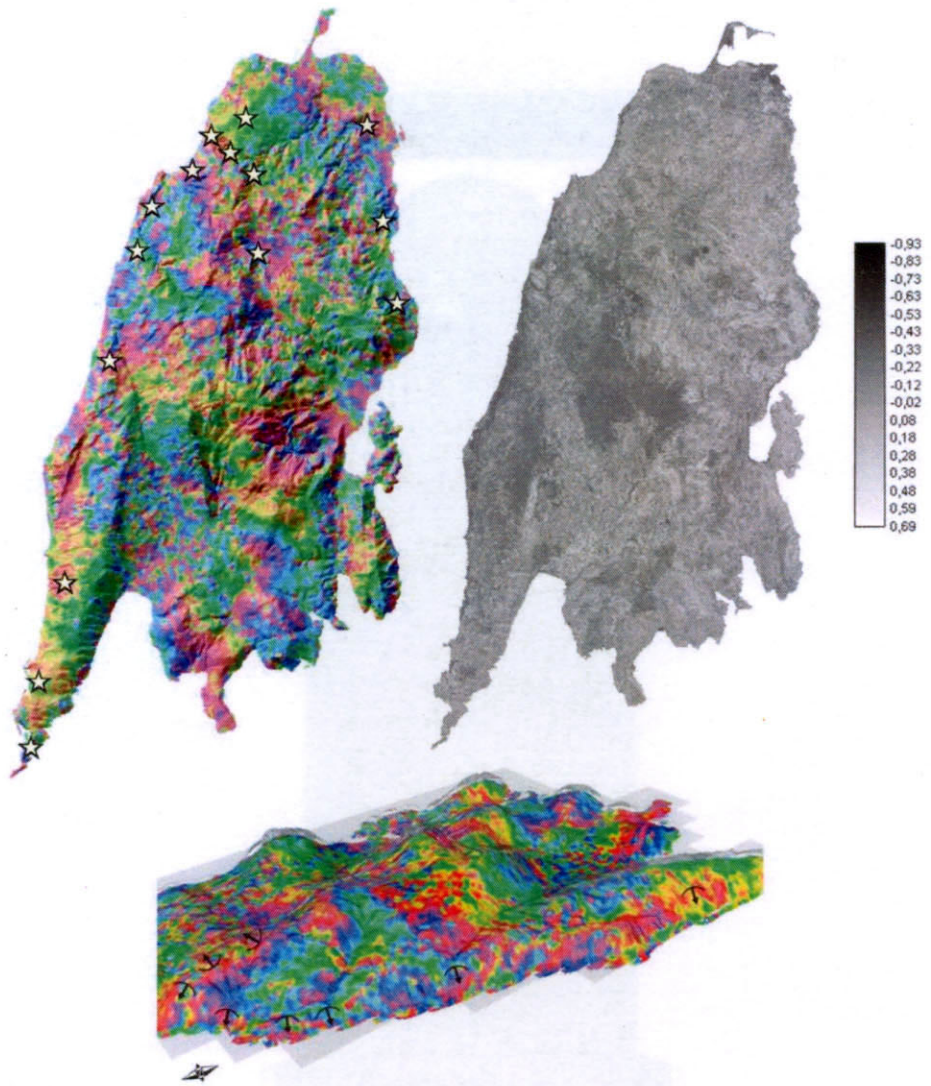

Fig. 4. Locations of rockfalls and landslides (stars) over the geocoded differential interferogram (top left), the NDVI index of the Lefkada island (top right) and a 3D-view of the maximum deformed area with the directions of slides (bottom).

Provided that the described geometric and processing parameters offer a good basis for the production of high quality InSAR results, taken in consideration also the magnitude of the event, the causes of the interferometric fringes degradation should be search to secondary geodynamic phenomena that accompanied the seismic event. As revealed by field observation the majority of the triggered secondary phenomena (landslide, rockfalls and liquefactions) were concentrated at the western cost of the island as well as at its northern edge and spatially coincide with the location of maximum deformation revealed by InSAR.
In conclusion, areas where the geological background and morphological characteristics favor the appearance of extensive secondary geodynamic phenomena, provided that the magnitude of the earthquake could trigger such gravity

movements, will show low interferometric coherence and as a consequence degradation of the observed fringe patterns. Accurate recognition on field of areas where ground failures occur could contribute to the interpretation of interferometric results, on the other hand a degradated interferometric fringe pattern could indicate among other factors areas where secondary phenomena take place.

5 ACKNOWLEDGEMENTS

The authors would like to acknowledge the Assistant Professor S. Lozios from the Dept. of Dynamic Tectonic & Applied Geology for his contribution during field work.

6 REFERENCES

1. Parcharidis Is. and Foumelis M., On the Assessment of Co-Seismic InSAR Images of Different Time Span Associated to Athens (Greece) 1999 Earthquake, *IGARSS 2005*, Vol. 7, 5251 5254, 2005.
2. Hanssen R., Satellite radar interferometry for deformation monitoring: a priori assessment of feasibility and accuracy. Intern. *Journal of Applied Earth Observation and Geoinformation*, Vol. 6, 253 260, 2005.
3. Peltzer G. et al., Analysis of coseismic surface displacement gradients using radar interferometry - new insights into the Landers earthquake, *Journal of Geophysical Research-Solid Earth*, Vol. 99, Iss. b11, 21971 21981, 1994.
4. Peltzer G.et al., The Mw 7.1, Hector Mine, California earthquake: surface rupture displacement field, and fault slip solution from ERS SAR data, *Earth and Planetary Sciences*, Vol. 333, 545 555, 2001.
5. Massonnet D. and. Feigl K.L., Radar interferometry and its application to changes in the earth's surface, *Rev. Geophys.*, Vol. 36, Is. 4, 441 500, 1998.
6. Wright T. et al., Measurement of interseismic strain accumulation across the North Anatolian fault by satellite radar interferometry, *Geophys. Res. Let.*, Vol. 28, Is. 10, 2117 2120, 2001.
7. Parcharidis Is. et al., Seismotectonic investigation on the Bam earthquake prone area (Iran) based on ASAR interferometry, *Proceedings of 2nd Intern. Conference on Recent Advances in Space Technologies*, 673 677, 2005.
8. McKenzie D.P., Active tectonics of the Alpine-Himalayan belt: The Aegean Sea and Surrounding regions, *Geuphs. J. R. Astr.*, SW. 55, 2 I7 254, 1978.
9. Kahle H. et al., The strain field in northwestern Greece and the Ionian Islands: results inferred from GPS measurements, *Tectonophysics,* Vol. 249, 41 52, 1995.
10. Cocard, M. et al., New constraints on the rapid crustal motion of the Aegean region: recent results inferred from GPS measurements (1993-1998) across the West Hellenic Arc, Greece, *E.P.S.L*, Vol. 172, 39 47, 1999.
11. Kiratzi A. and Langston C., Moment tensor inversion of January 17, 1983 Kefallinia event, Ionian islands (Greece), *Geophys. J. Int.*, Vol. 105, 529 535, 1999.
12. Louvari E. et al., The Cephallonia transform fault and its continuation to western Lefkada Island, *Tectonophysics*, Vol. 308, 223 236, 1999.
13. Hatzfeld D. et al., Microseismicity and strain pattern in north-western Greece, *Tectonics*, Vol. 14, 773 785, 1995.
14. Baker C. et al., Earthquake mechanisms of the Adriatic Sea and western Greece, *Geophys. J. Int,* Vol 131, 559 594, 1997.
15. Kiratzi A. and Louvari, E., Focal mechanisms of shallow earthquakes in the Aegean Sea and the surrounding lands determined by waveform modeling: A new database, *J. Geodyn.,* Vol. 36, 251 274, 2003.
16.Papazachos B. and Papazachou C., The earthquakes of Greece, Ziti Public, Thessaloniki, Greece, 2003.
17. Benetatos C. et al., The 14 Augoust 2003 Lefkada Island (Greece) earthquake: Focal mechanisms of the mainshocks and of the aftershock sequence, *J. Seis*, Vol. 9, 171 190, 2005.
18. Papathanassiou G. et al., The 2003 Lefkada earthquake: Field observations and preliminary microzonation map based on liquefaction potential index for the town of Lefkada, *Eng. Geol.*, Vol. 82, 12 31, 2003.
19. EERI Special Earthquake Report, Preliminary observations on the August 14, 2003, Lefkada Island (western Greece) earthquake, 1 12, 2003.